He *et al. J Wood Sci* (2020) 66:38
https://doi.org/10.1186/s10086-020-01886-z

Journal of Wood Science

ORIGINAL ARTICLE Open Access

Bending, shear, and compressive properties of three- and five-layer cross-laminated timber fabricated with black spruce

Minjuan He, Xiaofeng Sun, Zheng Li* and Wei Feng

Abstract

Cross-laminated timber (CLT) is an innovative engineering wood product made by gluing layers of solid-sawn lumber at perpendicular angles. The commonly used wood species for CLT manufacturing include spruce-pine-fir (SPF), douglas fir-larch, and southern pine lumber. With the hope of broadening the wood species for CLT manufacturing, the purposes of this study include evaluating the mechanical properties of black spruce CLT and analyzing the influence of CLT thickness on its bending or shear properties. In this paper, bending, shear, and compressive tests were conducted respectively on 3-layer CLT panels with a thickness of 105 mm and on 5-layer CLT panels with a thickness of 155 mm, both of which were fabricated with No. 2-grade Canadian black spruce. Their bending or shear resisting properties as well as the failure modes were analyzed. Furthermore, comparison of mechanical properties was conducted between the black spruce CLT panels and the CLT panels fabricated with some other common wood species. Finally, for both the CLT bending panels and the CLT shear panels, their numerical models were developed and calibrated with the experimental results. For the CLT bending panels, results show that increasing the CLT thickness whilst maintaining identical span-to-thickness ratios can even slightly reduce the characteristic bending strength of the black spruce CLT. For the CLT shear panels, results show that increasing the CLT thickness whilst maintaining identical span-to-thickness ratios has little enhancement on their characteristic shear strength. For the CLT bending panels, their effective bending stiffness based on the Shear Analogy theory can be used as a more accurate prediction on their experiment-based global bending stiffness. The model of the CLT bending specimens is capable of predicting their bending properties; whereas, the model of the CLT shear specimens would underestimate their ultimate shear resisting capacity due to the absence of the rolling shear mechanism in the model, although the elastic stiffness can be predicted accurately. Overall, it is attested that the black spruce CLT can provide ideal bending or shear properties, which can be comparable to those of the CLT fabricated with other commonly used wood species. Besides, further efforts should focus on developing a numerical model that can consider the influence of the rolling shear mechanism.

Keywords: Cross-laminated timber, Bending and shear property, Effect of thickness, Properties comparison, Numerical analysis

Introduction

Cross-laminated timber (CLT) is one kind of prefabricated engineered wood products, made of at least three orthogonal cross-wise layers of graded sawn lumber that are laminated by gluing with structural adhesives [1, 2]. Compared to other commonly used engineered wood products, CLT panels can perform with the advantages of higher in-plane compressive strength and stiffness, better acoustic and thermal performance, better integrity, etc. These advantages make the CLT panels pretty suitable and competitive for constructing mid- and high-rise timber buildings.

*Correspondence: zhengli@tongji.edu.cn
Department of Structural Engineering, Tongji University, Shanghai 200092, China

Since CLT has illustrated its potentials and competitiveness of using as dominant building materials for the mid- and high-rise timber buildings, a series of studies have focused on comprehending the mechanical properties (e.g., bending, rolling shear, compression, tension, etc.) of CLT panels based on tests. He et al. [3] tested the bending and compressive properties of CLT panels made from Canadian hemlock, and calibrated the theoretical bending stiffness using the experimental values. Sikora et al. [4] tested the bending and shear properties of three- and five-layer CLT panels fabricated with Irish Sitka spruce. It was attested that the bending or rolling shear strength decreased with an increase of the CLT thickness. Navaratnam et al. [5] tested both the bending and shear properties of CLT fabricated with Australian Radiate pine; furthermore, one numerical model for predicting its mechanical properties was developed. It highlighted that the shear strength could not be enhanced with an increase of the CLT thickness. Li [6] tested the rolling shear properties of CLT fabricated with New Zealand Radiata pine, and found that the lamination thickness affected its rolling shear strength significantly. Ukyo et al. [7] tested the rolling shear properties of CLT fabricated with Japanese cedar, and found that its rolling shear strength was highly correlated with the shear modulus. Oh et al. [8] proposed a lamina-property-based model for predicting the compressive strength of CLT panels, and revealed that the CLT compressive strength increased with an increase of the lamina number. Ido et al. [9] analyzed the effects of width and layups on the CLT tensile strength, and found that the tensile strength calculated using the Young's modulus of the lamina of each layer was in agreement with the measured tensile strength.

As for the numerical analysis on CLT panels, different methods can be applied for simulating the mechanical behaviors of CLT panels. Chen et al. [10] developed an orthotropically elastic model with different strengths in compression and tension for modeling work of timber structures; furthermore, Chen et al. [11] developed a constitutive model named Woodst combining a number of mechanics-based sub-models for numerical simulation of wood-based materials under forces and fire. It is proven capable of simulating the thermo-mechanical response of timber beams or glulam connections under force and fire. Ceccotti [12] and Franco et al. [13] studied the in-plane properties of CLT panels. In their CLT models, a set of elastic truss elements combined with nonlinear spring elements were used for simulating the CLT panels. D'Arenzo et al. [14] and Wilson et al. [15] studied the in-plane elastic properties of CLT floor diaphragms and the compressive plastic properties of CLT wall panels, respectively. In their CLT models, two-dimensional shell elements were used for simulating the CLT panels; furthermore, more complicated shell elements (e.g., ShellMIC4 element within OpenSees [16]) can be used to simulate the mechanical behavior of CLT, when the layup of the CLT panels should be considered. For achieving higher calculation accuracy, three-dimensional solid elements can be used to simulate the in-plane and out-of-plane behaviors of CLT panels. For instance, Hashemi et al. [17] investigated the compressive stress distribution within the CLT laminations using linear hex-structured shape elements. He et al. [3] developed one predictive model for 5-layer CLT bending panels using 8-node solid elements (i.e., SOLID45 element within ANSYS [18]).

A series of experimental research and theoretical analysis have been conducted for comprehending the mechanical properties of CLT panels [19]; whereas, systematical experimental research for comprehending the effect of CLT thickness on its out-of-plane bending or out-of-plane shear properties is still limited. Furthermore, few studies provide one modeling method for developing a reliable numerical model that can predict the CLT bending or shear behaviors. In this work, comprehensive bending tests as well as shear tests on both 3- and 5-layer CLT panels fabricated with Canadian black spruce (Picea mariana) were conducted. For the black spruce CLT panels, the effects of the thickness on their bending properties and on their shear properties were analyzed, respectively. Comparison of mechanical properties was conducted comprehensively between the black spruce CLT panels and the CLT panels fabricated with some other common wood species; besides, for the CLT bending specimens, comparison between their experimental bending stiffness and their analytical bending stiffness (i.e., the effective bending stiffness) was also conducted. Finally, for both the CLT bending specimens and the CLT shear specimens, their numerical models were developed and then calibrated with the experimental results. The research can provide fundamental basis for comprehending the effect of CLT thickness on its bending or shear properties; furthermore, the summary on the mechanical properties of different types of CLT panels fabricated with various wood species can provide meaningful reference values for engineering design.

Materials and test methods

Materials and specimens

Both the 5-layer and the 3-layer CLT panels were manufactured with a width of 310 mm, using the No.2-grade Canadian black spruce lumber [20]. The fabrication of the CLT panels met the requirements of PRG 320 [1]. The 5-layer CLT panels were fabricated with 35/25/35/25/35 mm layups with a 155-mm total thickness (CL5/155); the lumber with a nominal cross-section

dimension of 140 mm × 35 mm and that with a nominal cross-section dimension of 140 mm × 25 mm were respectively used for the longitudinal laminations and transverse laminations. The 3-layer CLT panels were fabricated with 35/35/35 mm layups with a 105-mm total thickness (CL3/105); the 140 mm × 35 mm cross-section lumber was used for both the longitudinal and the transverse laminations. All the CLT panels were assembled in cold press using a polyurethane adhesive; furthermore, edge gluing was performed. The average moisture content of the lumber was 12.5% with a coefficient of variation (COV) of 9.0%. For releasing the stress and then reducing the chances of developing cracks when the moisture content declined, lumber shrinkage relief was introduced to these CLT panels by sawing, forming the relief kerfs in the longitudinal laminations (Fig. 1). A detailed introduction of the relief kerfs is provided in CLT Handbook [21]. The relief kerfs cannot be too wide or too deep because they may reduce the bonding area, and affect the panel capacity and fire performance. Based on the requirements from CLT Handbook [21], the height of the relief kerfs should be less than half of the lamination thickness; whilst, it should ensures that less than 10% of the lamination cross-section or 5% of the lamination width is removed. The details of both the 3-layer and the 5-layer black spruce CLT panels are listed in Table 1.

Material properties

Three-point bending tests on the dimensional lumber for gluing the CLT panels were conducted for obtaining their bending stiffness. The cross-section of the bending lumber was 35 mm × 35 mm (width × depth). The total length of the bending lumber was 900 mm, which should be larger than 25 times of the lumber thickness (i.e., 875 mm); the net span of the lumber for the three-point bending tests should be 750 mm. A constant displacement loading rate of 5.0 mm/min was applied on these bending specimens. Both the dimensions of the specimens and the loading configurations were determined based on the code GB/T 26899 [22]. Based on the test results, the average MOE of the No. 2-grade Canadian black spruce lumber in the parallel-to-grain direction ($E_{l,0}$) and that in the perpendicular-to-grain direction ($E_{l,90}$) were 10925.0 MPa with a COV of 9.2% and 993.2 MPa with a COV of 11.0%, respectively. Therefore, based on the equivalent stiffness method suggested by CLT Handbook [21] for multi-layer orthotropic materials (e.g., CLT), the in-plane MOE of the 3-layer CLT panels in major compressive direction ($E_{c3,0}$) and that in minor compressive direction ($E_{c3,90}$) were 7614.4 MPa and 4303.8 MPa, respectively; the in-plane MOE of the 5-layer CLT panels in major compressive direction ($E_{c5,0}$) and that in minor compressive direction ($E_{c5,90}$) were 6838.8 MPa and 3717.4 MPa, respectively. Based on the experimental results from the CLT manufacturer, the average compressive strength of the black spruce lumber in the parallel-to-grain direction ($f_{lc,0}$) and that in the perpendicular-to-grain direction ($f_{lc,90}$) were 28.7 MPa with a COV of 9.2% and 5.8 MPa with a COV of 10.4%, respectively. The material properties of the black spruce lumber are listed in Table 2. Furthermore, for comprehending the in-plane compressive properties of the 3- and 5-layer CLT panels in both the major strength and the minor strength directions, 72 rectangular specimens with a sampling area of 100 mm × 100 mm were respectively extracted from the 3-layer CLT panels and from the 5-layer CLT panels; the thickness of these extracted rectangular specimens was equal to that of the 3-layer or

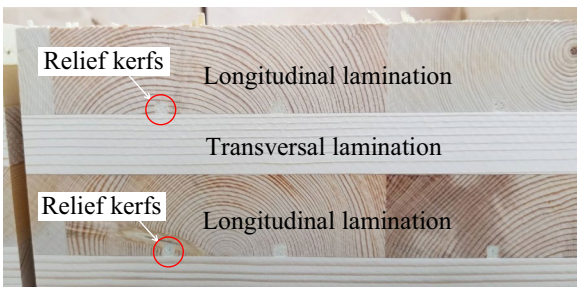

Fig. 1 Relief kerfs sawed in the CLT longitudinal laminations

Table 2 Material properties of the black spruce lumber

Properties	Canadian black spruce lumber	
	Parallel-to-grain direction	Perpendicular-to-grain direction
Stiffness (MPa), $E_{l,0}$ and $E_{l,90}$	10925.0	993.2
Strength (MPa), $f_{lc,0}$ and $f_{lc,90}$	28.7	5.8

Table 1 Details of the black spruce CLT panels

Type	Lumber grade	Lamination layups (mm)	Width (mm)	Average density (kg/m^3)
CL3/105	No.2	35/35/35	310	490 (9.0% COV)
CL5/155	No.2	35/25/35/25/35	310	486 (8.0% COV)

5-layer CLT panels, as shown in Fig. 2. These 72 extracted rectangular specimens were divided into two groups, with one group of 36 specimens tested for the major in-plane compressive properties, and the other group of 36 specimens tested for the minor in-plane compressive properties. Considering the discreteness of wood properties, the number of 36 per group was determined based on GB/T 50329 [23], which specified that at least 30 specimens were required for one group of compressive tests on timber.

Bending test method

Totally ten 3300-mm-length 3-layer black spruce CLT panels with 35/35/35 mm layups (CL3/105/3300) were tested for comprehending the bending performance in the major strength direction; whereas ten 4800-mm-length 5-layer black spruce CLT panels with 35/25/35/25/35 mm layups (CL5/155/4800) were tested for comprehending the bending performance in the major strength direction. Both the 3-layer and the 5-layer CLT panels with a width of 310 mm were fabricated with the lumber in the outermost laminations running parallel to the span direction. Since the distance between the support and the nearest end of the panel accounted for half of the CLT thickness, for the 3-layer CLT bending panels and for the 5-layer CLT bending panels, their span-to-thickness ratios were 30.4 and 30.0, respectively. Both the width and the span-to-thickness ratio were determined based on ANSI/APA PRG 320 [1], which specified a span-to-thickness ratio of 30 and a width larger than 305 mm for CLT bending specimens. For the CLT bending tests (taking the 5-layer CLT bending specimens as an example), the loading configurations (i.e., moment-critical configurations) of a four-point bending test determined based on prEN 16351 [24] are shown in Fig. 3a. Two loading points with a distance equal to six times of the CLT thickness h were applied to the central span of the bending specimens. A constant displacement loading rate of 6.4 mm/min was applied on the CLT bending specimens. Furthermore, for measuring both the local displacement and the global displacement of the CLT bending specimens, as recommended by EN 408 [25], four linear voltage displacement transducers (LVDTs 1-4) were used in each CLT bending specimen. The LVDTs 1–2 positioned in the mid-span on both sides of the bending specimens were used to measure the global displacements that could reflect both the bending and the shear mechanisms. The average displacement measured from the LVDTs 1–2 was namely the global displacement of the CLT bending specimens. The LVDTs 3–4 positioned in the neutral axis

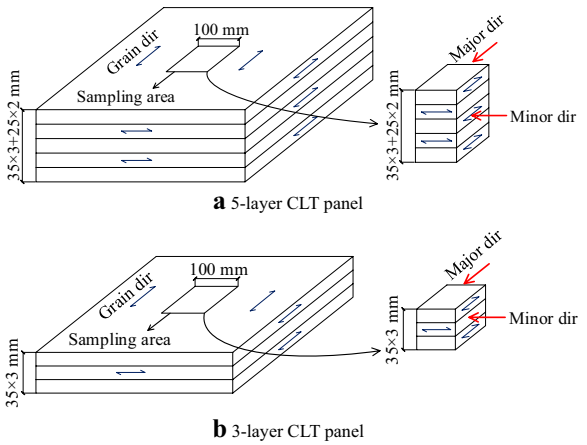

Fig. 2 Rectangular specimens extracted from the 3- or 5-layer CLT panels

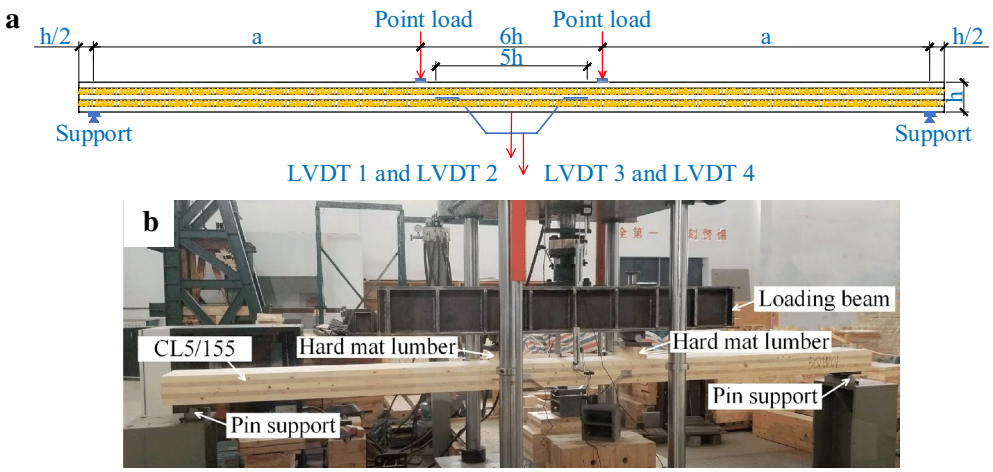

Fig. 3 The CLT bending specimen (5-layer CLT): **a** loading configurations; **b** bending test setup

on both sides of the bending specimens with a central gauge length of 5*h* were used to measure the displacements corresponding to the shear-free zone (Fig. 3a). Actually, the relative vertical displacement between the ends of the shear-free zone and the mid-span of the entire CLT bending specimen is the local displacement reflecting the pure bending mechanism. In this study, the local displacement was calculated by deducting the average displacement measured from the LVDTs 3–4 from the global displacement. The bending test setup is shown in Fig. 3b. The details of the CLT bending specimens are listed in Table 3.

Shear test method

Totally ten 680-mm-length 3-layer black spruce CLT panels with 35/35/35 mm layups (CL3/105/680) were tested for comprehending the shear performance in the major strength direction; whereas ten 1000-mm-length 5-layer black spruce CLT panels with 35/25/35/25/35 mm layups (CL5/155/1000) were tested for comprehending the shear performance in the major strength direction. Both the 3-layer and the 5-layer CLT panels with a width of 310 mm were fabricated with the lumber in the outermost laminations running parallel to the span direction. For the 3-layer or the 5-layer CLT shear panels, their span-to-thickness ratios were 5.5, which was determined based on ANSI/APA PRG 320 [1] specifying a span-to-thickness ratio between 5 and 6. One loading point with a constant displacement loading rate of 6.4 mm/min was applied in the mid-span of the CLT shear specimens (taking the 5-layer CLT shear specimen as an example), as shown in Fig. 4a. The LVDTs 1–2 were positioned in the mid-span on both sides of the CLT shear specimens, and the average displacement measured from the LVDTs 1–2 was namely the shear deformation. The shear test setup is shown in Fig. 4b. The details of the CLT shear specimens are listed in Table 4.

Table 3 Details of CLT bending specimens

Specimen label	No. of specimens	No. of layers	Thickness (mm)	Span (mm)	Width (mm)	Loading configuration	Target properties
CL3/105/3300	10	3	105	3300	310	Two out-of-plane loading points	Bending strength & stiffness
CL5/155/4800	10	5	155	4800	310	Two out-of-plane loading points	Bending strength & stiffness

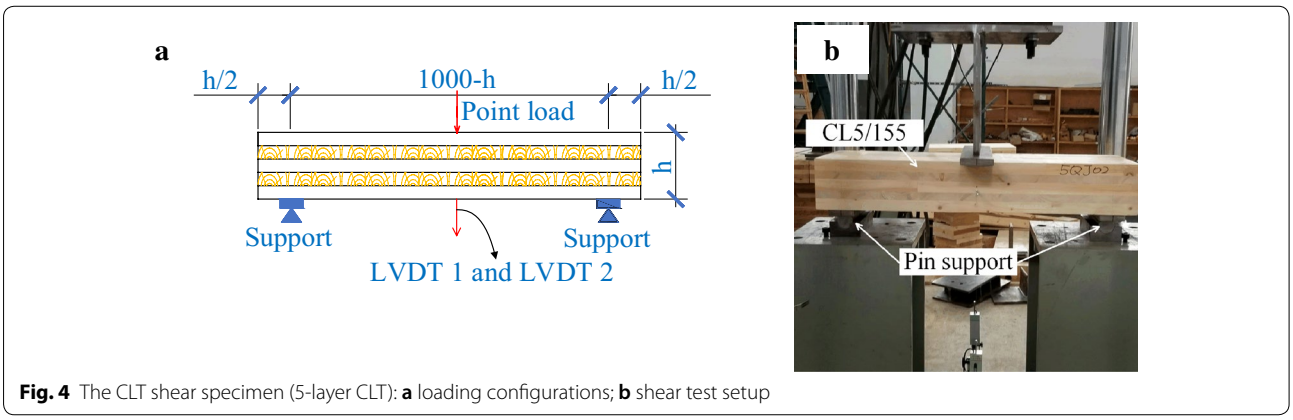

Fig. 4 The CLT shear specimen (5-layer CLT): **a** loading configurations; **b** shear test setup

Table 4 Details of CLT shear specimens

Specimen label	No. of specimens	No. of layers	Thickness (mm)	Span (mm)	Width (mm)	Loading configuration	Target properties
CL3/105/680	10	3	105	680	310	One out-of-plane loading point	Shear strength & stiffness
CL5/155/1000	10	5	155	1000	310	One out-of-plane loading point	Shear strength & stiffness

Results and discussion

Compressive test

Based on the compressive tests on the aforementioned rectangular specimens extracted from the 3-layer or the 5-layer CLT panels, the major or minor compressive stress–strain relationships for both the 3-layer and the 5-layer CLT panels are obtained (Fig. 5). For the 3-layer CLT panels, the average in-plane major compressive strength ($f_{c3,0}$) and the average in-plane minor compressive strength ($f_{c3,90}$) were 21.1 MPa with a COV of 6.7% and 13.4 MPa with a COV of 9.8%, respectively. For the 5-layer CLT panels, the average in-plane major compressive strength ($f_{c5,0}$) and the average in-plane minor compressive strength ($f_{c5,90}$) were 23.5 MPa with a COV of 6.0% and 14.7 MPa with a COV of 6.5%, respectively. In the major or minor compressive direction, the in-plane compressive strength of the CLT panels increases slightly with an increase of the CLT thickness. It is found that the ratio of the $f_{c3,0}$ to the $f_{c5,0}$ (i.e., 0.90) or that of the $f_{c3,90}$ to the $f_{c5,90}$ (i.e., 0.92) is similar to the ratio between $(t_1+t_3)/(t_1+t_2+t_3)$ of the 3-layer CLT and $(t_1+t_3+t_5)/(t_1+t_2+t_3+t_4+t_5)$ of the 5-layer CLT (t_i is the thickness of lamination i). Such a relation was stated by Chen et al. [26]. Furthermore, the $f_{c3,90}$ or the $f_{c5,90}$ is more than twice of the perpendicular-to-grain compressive strength of the lumber ($f_{lc,90}$). It is partly due to the reason that the cross-laminated structure restrains the horizontal expansion in the laminations under vertical compression, thus enhancing the minor compressive strength of CLT. The enhancing effect increases with the number of the CLT layers [26]. Furthermore, the in-plane MOEs of the CLT panels calculated following the equivalent stiffness method are slightly larger than those estimated from the stress–strain relationships shown in Fig. 5. It is because of the gap existing along the interface between the loading plates and the rectangular specimens, which can cause larger measurements of the compressive deformation for these rectangular specimens, and therefore less in-plane MOEs based on the stress–strain relationships. The in-plane MOEs calculated following the equivalent stiffness method are more accurate. The material properties of both the 3-layer and the 5-layer CLT panels are listed in Table 5.

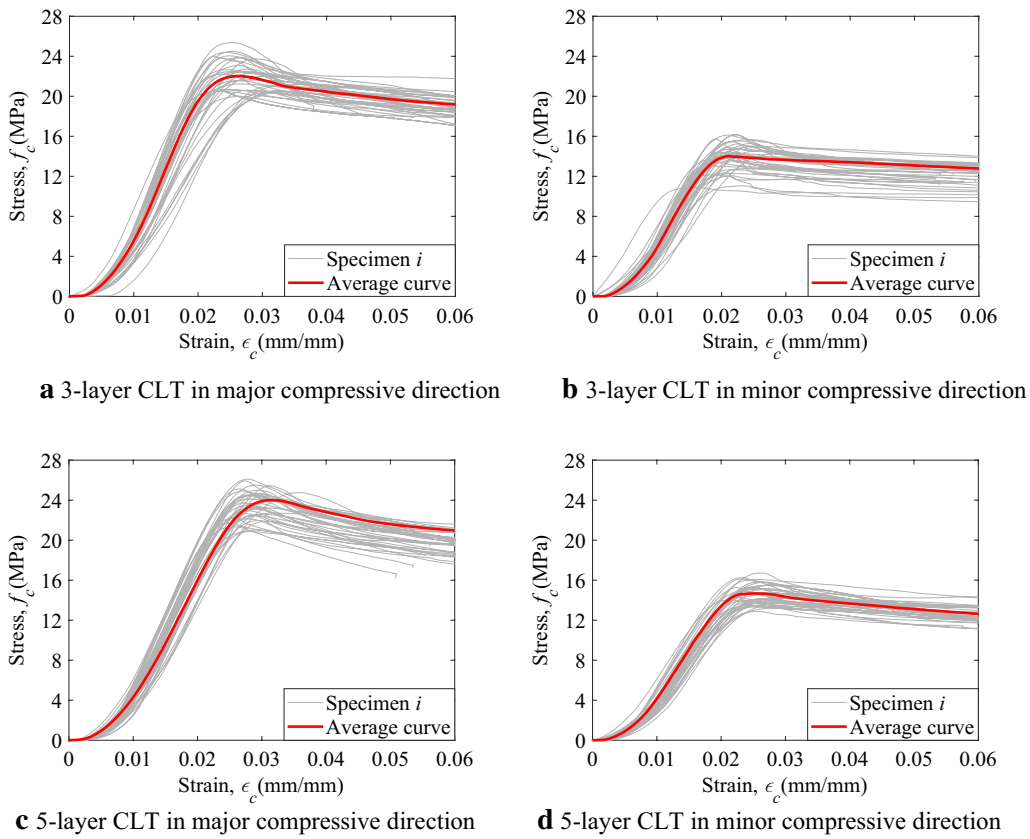

a 3-layer CLT in major compressive direction

b 3-layer CLT in minor compressive direction

c 5-layer CLT in major compressive direction

d 5-layer CLT in minor compressive direction

Fig. 5 Stress–strain relationship for CLT panels under in-plane compression

Table 5 Compressive properties of the CLT panels

Properties	3-layer CLT, CL3/105	
	Parallel-to-grain direction	Perpendicular-to-grain direction
Stiffness (MPa), $E_{c3,0}$ and $E_{c3,90}$	7614.4	4303.8
Strength (MPa), $f_{c3,0}$ and $f_{c3,90}$	21.1	13.4
	5-layer CLT, CL5/155	
Stiffness (MPa), $E_{c5,0}$ and $E_{c5,90}$	6838.8	3717.4
Strength (MPa), $f_{c5,0}$ and $f_{c5,90}$	23.5	14.7

Bending test

For the CLT bending specimens, both the local bending stiffness ($EI_{m,l}$) and the global bending stiffness ($EI_{m,g}$) can be calculated respectively based on Eqs. (1) and (2) originally from EN 408 [25] and further modified by Christovasilis et al. [27] for CLT; in Eq. (1), a is the distance between the loading head and the nearest support, l_1 is equal to the gauge length for the local displacement measurement (i.e., $5h$), F_1 and F_2 are respectively 10% and 40% of the ultimate load-resisting capacity ($F_{\max}$), and w_1 and w_2 are the local displacements corresponding to the F_1 and the F_2, respectively; whereas, in Eq. (2), w_1 and w_2 are the global displacements corresponding to the F_1 and the F_2, l is the span between the supports. The effective shear stiffness GA_{eff} can be calculated using Eq. (3), in which b_i and h_i are the width and the thickness of lamination i, respectively; G_i represents the shear modulus parallel to grain (G_0) for longitudinal laminations and represents the rolling shear modulus (G_{90}) for transverse laminations, respectively. K is the shear correlation factor, which was adopted as 0.23 in this study for common layups [28]. For the tested black spruce CLT panels, G_0 and G_{90} were adopted as 682.8 MPa and 68.3 MPa, respectively, based on the definitions from EN 338 [29] (i.e., $G_0 = E_{l,0}/16$, $G_{90} = G_0/10$).

$$EI_{m,l} = \frac{a \cdot l_1^2 \cdot (F_2 - F_1)}{16(w_2 - w_1)} \tag{1}$$

$$EI_{m,g} = \frac{3al^2 - 4a^3}{48\left(\frac{w_2 - w_1}{F_2 - F_1} - \frac{a}{2GA_{\text{eff}}}\right)} \tag{2}$$

$$GA_{\text{eff}} = \kappa \cdot \sum_i G_i \cdot b_i \cdot h_i \tag{3}$$

For the 3-layer black spruce CLT bending specimens, the relations between the load versus the average displacement from LVDTs 1–2 (i.e., global displacement) as well as the relations between the load versus the average displacement from LVDTs 3–4 are shown in Fig. 6a, b, respectively. For each CLT bending specimen, the global displacement corresponding to $F_{\max}$ is approximately 5.6 mm larger than the corresponding average displacement from the LVDTs 3–4. The gap between the average displacement from the LVDTs 1–2 and the average

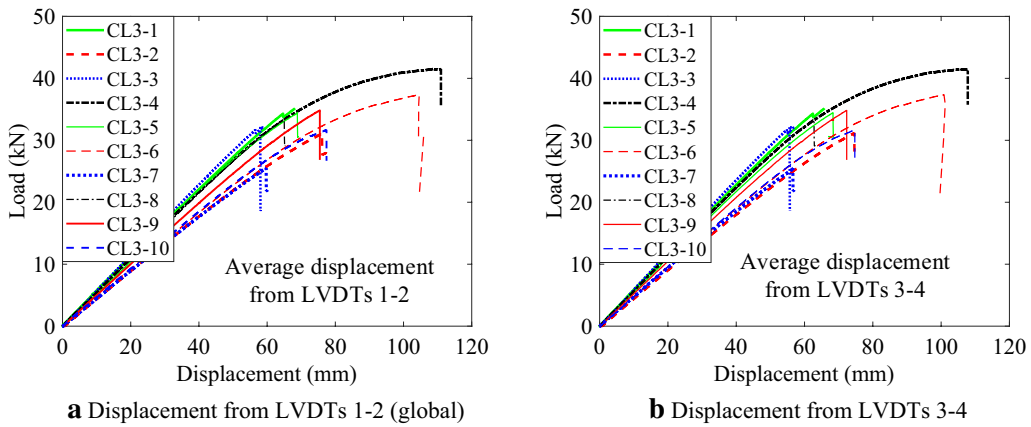

a Displacement from LVDTs 1-2 (global) **b** Displacement from LVDTs 3-4

Fig. 6 The 3-layer CLT bending specimens

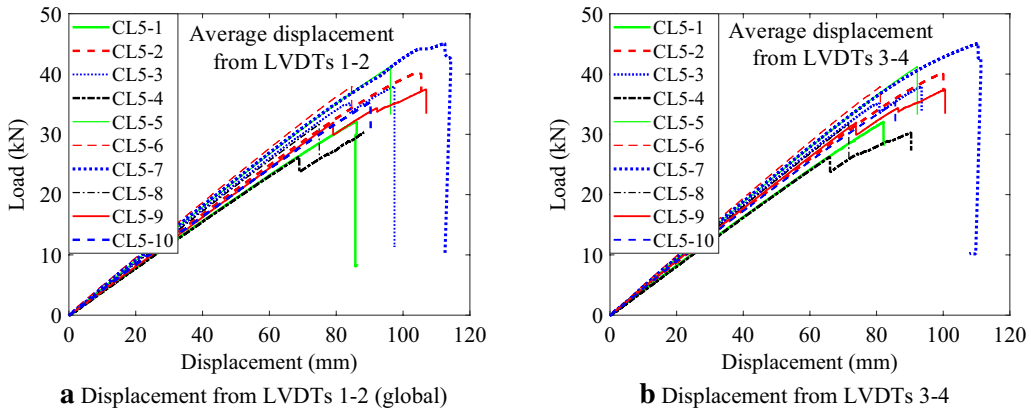

a Displacement from LVDTs 1-2 (global) **b** Displacement from LVDTs 3-4

Fig. 7 The 5-layer CLT bending specimens

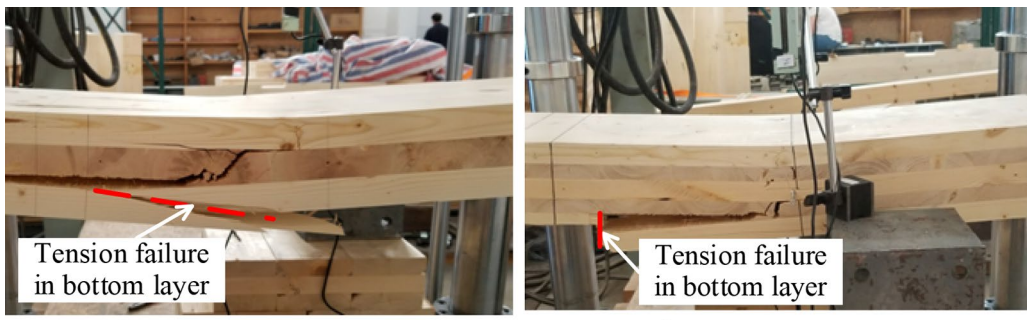

a 3-layer CLT panel **b** 5-layer CLT panel

Fig. 8 Failure modes of the CLT bending panels

displacement from the LVDTs 3–4 is namely the local displacement for the 3-layer CLT bending specimens. For the 5-layer black spruce CLT bending specimens, the relations between the load versus the average displacement from LVDTs 1–2 (i.e., global displacement) as well as the relations between the load versus the average displacement from LVDTs 3–4 are shown in Fig. 7a, b, respectively. When the load reaches F_{max}, the gap between the average displacement from the LVDTs 1–2 (i.e., global displacement) and the average displacement from the LVDTs 3–4 is around 3.0 mm, which is namely the local displacement for the 5-layer CLT bending specimens.

For both the 3-layer and the 5-layer black spruce CLT bending specimens, the dominant failure mode is the brittle tension failure occurring in the CLT bottom longitudinal laminations, as shown in Fig. 8. Furthermore, for one 3-layer CLT bending specimen with a finger joint located in the bottom longitudinal lamination close to the mid-span, the finger joint zone is prone to the brittle tension failure, as shown in Fig. 9.

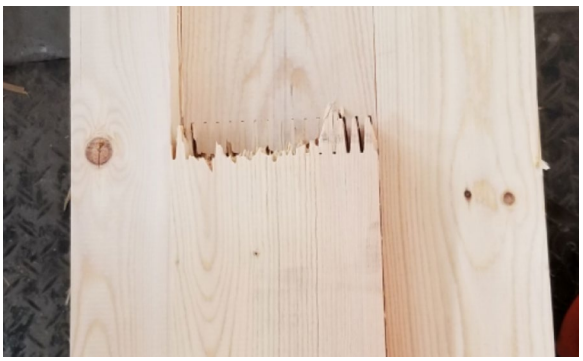

Fig. 9 Finger joint damages occurring in the CLT bottom lamination

Therefore, for CLT manufacturers, special attentions should be paid to the location of the finger joints, which should be remained an enough distance from the mid-span of CLT bending components. Furthermore, it should be noted that the finger joint effect maybe pronounced when the original CLT panel is divided into several ones with smaller width (e.g., 310 mm). For the

fabricated CLT panels satisfying the requirements from PRG 320 [1], this failure mode can be avoided.

For the 3-layer or the 5-layer black spruce CLT bending specimens, their characteristic bending strength (f_b) can be calculated using Eq. (4) based on the *Timoshenko Beam* theory [27, 30], in which M_{max} is the maximum bending moment. S_{eff} is the effective section modulus calculated using Eq. (5), in which $EI_{m,l}$ is the local bending stiffness representing the pure bending mechanism; h is the CLT thickness; E_1 is the MOE of the CLT outermost laminations (i.e., $E_1 = E_{l,0} = 10925$ MPa).

$$f_b = \frac{M_{max}}{S_{eff}} \tag{4}$$

$$S_{eff} = \frac{EI_{m,l}}{E_1 \cdot h/2} \tag{5}$$

Based on these aforementioned Eqs. (1)–(5), the bending properties of both the 3-layer CLT panels and the 5-layer CLT panels can be calculated, as listed in Tables 6 and 7. For the 3-layer CLT bending panels fabricated with No.2-grade black spruce, the average

Table 6 Experimental results for 3-layer CLT bending panels (CL3/105/3300)

No.	Load (kN)		Global disp. (mm)		Local disp. (mm)		F_{max} (kN)	Global K_e (N/mm), $(F_2\text{-}F_1)/(W_2\text{-}W_1)$	Experimental bending stiffness, x 10^{11} (N mm^2)		S_{eff}, x 10^5 (mm^3)	f_b (MPa)
	F_1	F_2	W_1	W_2	W_1	W_2			$EI_{m,l}$	$EI_{m,g}$		
1	3.513	14.052	6.065	25.010	0.129	0.670	35.130	556.295	4.304	3.970	7.5037	30.021
2	3.12	12.48	7.390	27.980	0.152	0.730	31.200	454.590	3.578	3.180	6.2377	32.074
3	3.217	12.868	5.785	22.470	0.255	0.730	32.170	578.424	4.489	4.146	7.8263	26.359
4	4.150	16.600	7.750	30.360	0.291	0.890	41.500	550.641	4.592	3.925	8.0060	33.240
5	3.446	13.784	6.748	26.480	0.297	0.800	34.460	523.921	4.541	3.715	7.9167	27.913
6	3.738	14.952	8.232	32.590	0.247	0.890	37.380	460.383	3.853	3.224	6.7178	35.681
7	2.548	10.192	5.730	22.770	0.444	0.940	25.480	448.592	3.405	3.134	5.9363	27.524
8	3.338	13.352	6.344	24.860	0.394	0.930	33.380	540.830	4.128	3.847	7.1964	29.744
9	3.484	13.936	6.986	27.580	0.276	0.880	34.840	507.526	3.823	3.587	6.6655	33.517
10	3.168	12.672	6.677	27.260	0.225	0.820	31.680	461.740	3.529	3.234	6.1526	33.018
Mean	3.372	13.49	6.771	26.736	0.271	0.828	33.722	508.294	4.024	3.596	7.0159	30.909
Cov	12.4%	12.4%	12.3%	11.9%	15.5%	11.3%	12.4%	9.5%	11.1%	10.5%	11.1%	9.8%

Table 7 Experimental results for 5-layer CLT bending panels (CL5/155/4800)

No.	Load (kN)		Global Disp. (mm)		Local Disp. (mm)		F_{max} (kN)	Global K_e (N/mm), $(F_2\text{-}F_1)/(W_2\text{-}W_1)$	Experimental bending stiffness, x 10^{11} (N mm^2)		S_{eff}, x 10^5 (mm^3)	f_b (MPa)
	F_1	F_2	W_1	W_2	W_1	W_2			$EI_{m,l}$	$EI_{m,g}$		
1	3.207	12.828	8.118	32.730	0.370	1.150	32.070	390.907	8.601	8.264	10.158	29.321
2	4.019	16.076	9.482	38.370	0.472	1.390	40.190	417.371	9.158	8.867	10.816	34.509
3	3.793	15.172	8.721	34.440	0.299	1.130	37.930	442.436	9.548	9.444	11.277	31.238
4	3.031	12.124	8.072	31.230	0.467	1.200	30.310	392.650	8.650	8.304	10.216	27.554
5	4.126	16.504	9.356	36.710	0.384	1.240	41.260	452.512	10.083	9.677	11.908	32.178
6	3.787	15.148	7.664	32.150	0.356	1.070	37.870	463.979	11.095	9.944	13.104	26.840
7	4.509	18.036	9.678	39.758	0.309	1.138	45.090	449.701	11.378	9.612	13.438	31.163
8	3.166	12.664	7.421	29.370	0.577	1.281	31.660	432.730	9.407	9.220	11.111	26.464
9	3.742	14.968	9.525	36.889	0.523	1.219	37.420	410.247	11.247	8.704	13.283	26.164
10	3.534	14.136	8.717	34.400	0.528	1.350	35.340	412.802	8.993	8.763	10.622	30.900
Mean	3.691	14.766	8.675	34.605	0.429	1.217	36.914	426.533	9.816	9.080	11.593	29.633
Cov	12.6%	12.6%	9.5%	9.6%	12.8%	8.3%	12.6%	6.0%	10.9%	6.5%	10.9%	9.5%

ultimate load-resisting capacity (F_{max}) is 33.722 kN (the range is 25.480–41.500 kN) with a COV of 12.4%. The average global initial elastic stiffness (K_e), which is the average slope ratio of those load–displacement curves shown in Fig. 6a, is 508.294 N/mm (the range is 448.592–578.424 N/mm) with a COV of 9.5%. The average local bending stiffness ($EI_{m,l}$) and the average global bending stiffness ($EI_{m,g}$) are 4.024×10^{11} N mm^2 (COV is 11.1%) and 3.596×10^{11} N mm^2 (COV is 10.5%), respectively. The average characteristic bending strength (f_b) is 30.909 MPa with a COV of 9.8%. In contrast, for the 5-layer CLT bending panels fabricated with No.2-grade black spruce, the average F_{max} is 36.914 kN (the range is 30.310–45.090 kN) with a COV of 12.6%. The average global K_e is 426.533 N/mm (the range is 390.907–463.979 N/mm) with a COV of 6.0%. The average $EI_{m,l}$ and the average $EI_{m,g}$ are 9.816×10^{11} N mm^2 (COV is 10.9%) and 9.080×10^{11} N mm^2 (COV is 6.5%), respectively. The average f_b is 29.633 MPa with a COV of 9.5%.

Shear test

In this study, the compressive deformation of the CLT shear specimens at the supports was ignored, which was extremely small (less than 1 mm). The dominant failure mode for both the 3-layer and the 5-layer CLT shear specimens is the rolling shear failure occurring in the transverse laminations, as shown in Fig. 10. Since de-lamination failure resulting from CLT manufacturing defects was observed in one 3-layer CLT shear specimen, which cannot reflect the typical shear mechanism of CLT panels, its experimental result was excluded from the shear properties analyses. Then, for the 9 3-layer CLT shear specimens and for the 10 5-layer CLT shear specimens, their load–displacement curves are shown in Fig. 11a ,b, respectively. The mid-span displacement is the average vertical displacement measured from the LVDTs 1–2, as shown in Fig. 4a. For the 3-layer CLT shear specimens, their average ultimate shear resisting capacity (FV_{max}) is 51.639 kN with a COV of 7.5%; for the 5-layer CLT shear specimens, their average FV_{max} is 69.806 kN with a COV of 5.6%. For both the 3-layer and the 5-layer CLT shear specimens, their characteristic shear strength (f_v) can be calculated using Eqs. (6) and (7) from CLT Handbook [21], in which $EI_{eff,shear}$ is the effective bending stiffness calculated based on the Shear Analogy theory; E_i represents $E_{l,0}$ for the longitudinal lamination and represents $E_{l,90}$ for the transverse lamination, respectively; h_i is the thickness of lamination i, except for the middle

a 3-layer CLT panel **b** 5-layer CLT panel

Fig. 10 Failure modes of CLT shear specimens

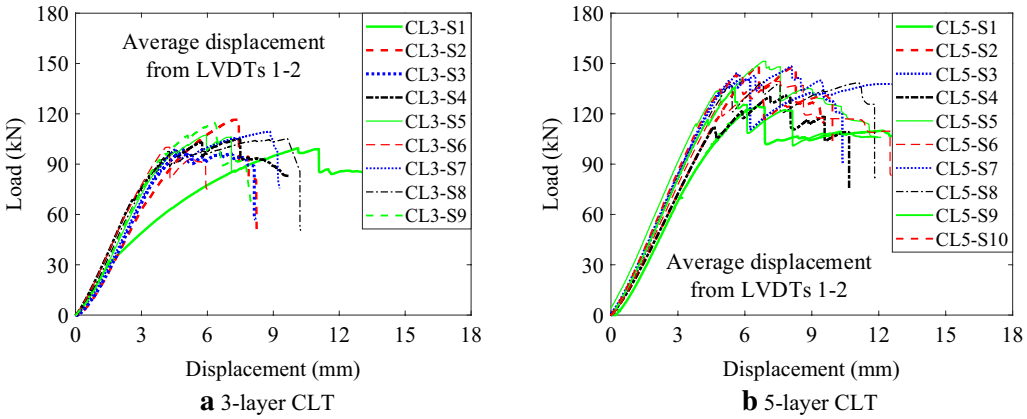

a 3-layer CLT **b** 5-layer CLT

Fig. 11 CLT shear tests

lamination, which is half of its thickness; z_i is the distance from the centroid of the lamination to the CLT neutral axis, except for the middle lamination, where it is to the centroid of the top half of that lamination. $EI_{\text{eff,shear}}$ can be calculated using Eq. (8), in which A_i is the cross-section area of lamination i. Whereas, compared to the $EI_{\text{eff,shear}}$, the $EI_{m,l}$ reflecting the pure bending mechanism of the specimens is more related to the CLT bending properties; furthermore, the experiment-based $EI_{m,l}$ can consider almost all affecting factors of bending stiffness. Therefore, in this paper, the $EI_{m,l}$ instead of the $EI_{\text{eff,shear}}$ was used in Eq. (6) for calculating the f_v of the CLT shear specimens. The experimental properties of both the 3-layer and the 5-layer CLT shear specimens are listed in Table 8. The average characteristic shear strength (f_v) of the 3-layer CLT panels is 1.737 MPa with a COV of 7.5%; in contrast, the average f_v of the 5-layer CLT panels is 1.803 MPa with a COV of 6.5%. Based on the definitions from ANSI/APA PRG 320 [1], the characteristic rolling shear strength (f_r) can be estimated as one-third of the characteristic shear strength (f_v). Therefore, for the 3-layer CLT panels and for the 5-layer CLT panels, their f_r is approximately 0.579 MPa and 0.601 MPa, respectively.

$$(Ib/Q)_{\text{eff}} = \frac{EI_{\text{eff,shear}}}{\sum_{i=1}^{n/2} E_i h_i Z_i} \tag{6}$$

$$FV_{\max} = f_v(Ib/Q_{\text{eff}}) \tag{7}$$

$$EI_{\text{eff,shear}} = \sum_{i=1}^{n} E_i \cdot b_i \cdot \frac{h_i^3}{12} + \sum_{i=1}^{n} E_i \cdot A_i \cdot z_i^2 \tag{8}$$

Table 8 Experimental results for CLT shear panels

	CL3/105/680		CL5/155/1000	
$EI_{m,l}$, × 10^{11} (N mm^2)	4.024		9.816	
$\sum E_i h_i Z_i$, × 10^7 (N)	1.354		2.536	
Ib/Q_{eff}, × 10^4 (mm^2)	2.973		3.871	
No.	$FV_{\max}$ (kN)	f_v (MPa)	$FV_{\max}$ (kN)	f_v (MPa)
1	49.775	1.674	62.537	1.616
2	58.344	1.962	74.175	1.916
3	49.611	1.669	70.164	1.813
4	47.607	1.601	65.521	1.693
5	53.609	1.803	75.711	1.956
6	50.114	1.686	69.940	1.807
7	49.520	1.666	71.689	1.852
8	48.772	1.640	68.694	1.775
9	57.395	1.931	67.831	1.752
10	–	–	71.803	1.855
Mean	51.639	1.737	69.806	1.803
COV	7.5%		5.6%	

Effect of thickness

For the 5-layer CLT panels with a thickness of 155 mm and for the 3-layer CLT panels with a thickness of 105 mm, their bending and shear properties are compared, as listed in Table 9. For those CLT bending specimens, the $F_{\max}$ of the 5-layer CLT panels is only 9.46% higher than that of the 3-layer CLT panels; furthermore, the f_b of the 5-layer CLT panels is even less than that of the 3-layer CLT panels. It indicates that increasing the CLT thickness whilst maintaining identical span-to-thickness ratios cannot enhance their ultimate load-resisting capacity $F_{\max}$. Besides, increasing the CLT thickness cannot enhance the characteristic bending strength f_b of the CLT panels with identical span-to-thickness ratios. It is because that the f_b of one CLT panel is mainly determined by the bending strength of the outermost lamination of the CLT. Similar findings were also reported by Sikora et al. [4] and Navaratnam et al. [5]. Furthermore, when the thickness of the outermost lamination of one CLT enhances, the f_b of the CLT panel would decrease, due to the size effect of the outermost lamination on its bending strength. The Global K_e (i.e., average slope ratio of those load–displacement curves) of the 5-layer CLT panels is 16.08% less than that of the 3-layer CLT panels, which means that increasing the CLT thickness whilst maintaining identical span-to-thickness ratios can weaken the global K_e of the CLT bending specimens. Although increasing the thickness from 3-layer CLT to 5-layer CLT has enhanced the moment of inertia

Table 9 Properties comparison between 3-layer CLT and 5-layer CLT

CLT configuration	Bending properties					Shear properties	
	$F_{\max}$ (kN)	GlobalK_e (N/mm)	$EI_{m,l}$ × 10^{11} (N mm^2)	$EI_{m,g}$ × 10^{11} (N mm^2)	f_b (MPa)	$FV_{\max}$ (kN)	f_v (MPa)
CL3/105	33.722	508.294	4.024	3.596	30.909	51.639	1.737
CL5/155	36.914	426.533	9.816	9.080	29.633	69.806	1.803

for the CLT cross-section; whereas, maintaining identical span-to-thickness ratios can simultaneously increase the span of the bending CLT, which is more dominant in weakening the slope ratio of CLT load–displacement curve (i.e., Global K_e). When the CLT configurations enhance from three laminations with a thickness of 105 mm to five laminations with a thickness of 155 mm, the local bending stiffness $EI_{m,l}$ and the global bending stiffness $EI_{m,g}$ increase by 145.0% and 152.0%, respectively; therefore, for those CLT bending specimens, increasing their thickness can enhance their $EI_{m,l}$ or $EI_{m,g}$ significantly.

For those CLT shear specimens, the $FV_{\max}$ of the 5-layer CLT panels with a thickness of 155 mm is 35.18% higher than that of the 3-layer CLT panels with a thickness of 105 mm. Therefore, increasing the CLT thickness whilst maintaining identical span-to-thickness ratios can have a significant enhancement on its ultimate shear-resisting capacity $FV_{\max}$; whereas, that arrangement has little enhancement on its characteristic shear strength f_v, because the f_v of the 5-layer CLT shear panels is only 3.8% higher than that of the 3-layer CLT shear panels. It is because the f_v of one CLT panel is mainly determined by the shear strength of the transverse laminations of the CLT. The f_v of the 3-layer CLT with 35-mm-thickness transverse laminations is slightly less than that of the 5-layer CLT with 25-mm-thickness transverse laminations, which is caused by the size effect of the transverse laminations on their shear strength.

Experimental and analytical bending stiffness

For the CLT bending specimens, their experiment-based bending stiffness (i.e., $EI_{m,l}$ and $EI_{m,g}$) can be estimated using the theoretical bending stiffness (i.e., effective bending stiffness EI_{eff}). The theory-based EI_{eff} can be calculated without the time- and energy-consuming bending tests; besides, EI_{eff} can be calculated directly using the geometric characteristics of CLT sections and the MOEs of CLT laminations, based on the Shear Analogy theory (i.e., $EI_{\text{eff,shear}}$) or the Modified Gamma theory (i.e., $EI_{\text{eff,Gamma}}$). The aforementioned Eq. (8) is used for calculating the $EI_{\text{eff,shear}}$. As for the $EI_{\text{eff,Gamma}}$, it can be calculated using Eq. (9) following the Modified Gamma theory, which stems from the Mechanically Jointed Beams theory or the Gamma theory [31] that takes no shear deformation into consideration, in which z_i is the distance from the centroid of the lamination to the CLT neutral axis; E_i is the MOE of lamination i; h_i and b_i are the thickness and width of lamination i, respectively; γ_i is the connection efficiency factor (non-zero only for the longitudinal laminations and equal to unity for the middle lamination). γ_i can be calculated using Eq. (10), in which L_{eff} is the effective length of the beam, which is 3195 mm for the 3-layer CLT bending specimens and 4645 mm for the 5-layer CLT bending specimens, respectively; j is the transverse lamination connecting the ith longitudinal lamination with the central lamination. As mentioned above, the rolling shear modulus G_{90} (i.e., the shear modulus of the transverse laminations) was adopted as 68.3 MPa. Therefore, for the 3-layer CLT bending specimens and for the 5-layer CLT bending specimens, their $EI_{\text{eff,shear}}$ was calculated as 3.157×10^{11} N mm^2 and 9.044×10^{11} N mm^2, respectively; their $EI_{\text{eff,Gamma}}$ was calculated as 2.654×10^{11} N mm^2 and 8.532×10^{11} N mm^2, respectively.

$$EI_{\text{eff,Gamma}} = \sum_{i=1}^{n} E_i \cdot b_i \cdot \frac{h_i^3}{12} + \sum_{i=1}^{n} \gamma_i \cdot E_i \cdot b_i \cdot h_i \cdot z_i^2 \tag{9}$$

$$\gamma_i = \left(1 + \frac{\pi^2 \cdot E_i \cdot b_i \cdot h_i}{L_{\text{eff}}^2 \cdot \left(G_{90} \cdot b_j / h_j\right)}\right)^{-1} \tag{10}$$

For the 3-layer or the 5-layer CLT bending specimens, their experimental bending stiffness (i.e., $EI_{m,l}$ and $EI_{m,g}$) are compared with their theoretical bending stiffness (i.e., $EI_{\text{eff,shear}}$ and $EI_{\text{eff,Gamma}}$), as shown in Fig. 12. For the 3-layer CLT bending specimens, their $EI_{\text{eff,shear}}$ is 21.55% less than the average $EI_{m,l}$ and 12.21% less than the average $EI_{m,g}$, respectively; in contrast, their $EI_{\text{eff,Gamma}}$ is 34.05% less than the average $EI_{m,l}$ and 26.20% less than the average $EI_{m,g}$, respectively. For the 5-layer CLT bending specimens, their $EI_{\text{eff,shear}}$ is 7.86% less than the average $EI_{m,l}$ and 0.40% less than the average $EI_{m,g}$, respectively; in contrast, their $EI_{\text{eff,Gamma}}$ is 13.08% less than the average $EI_{m,l}$ and 6.04% less than the average $EI_{m,g}$, respectively. Therefore, for either the 3-layer CLT bending panels or the 5-layer CLT bending panels, their $EI_{\text{eff,shear}}$ is much closer to the $EI_{m,g}$, because the $EI_{\text{eff,shear}}$ based on the Shear Analogy theory takes both shear and flexural deformations into consideration. It indicates that the $EI_{\text{eff,shear}}$ can be used as a more accurate prediction on the $EI_{m,g}$ of the CLT bending panels.

Properties' comparison

The mechanical properties of CLT panels fabricated with different wood species are listed in Table 10, in which the flexural MOE (E_{b}) of the CLT bending specimens is calculated by dividing the local bending stiffness ($EI_{m,l}$) by the second moment of the cross-sectional inertia (I). Some findings can be concluded as: (1) the 3-layer CLT fabricated with No.2-grade black spruce lumber can provide the largest E_{b} among all the CLT types listed in Table 10; furthermore, their mechanical properties are even better than those of E1-grade CLT defined in ANSI/APA PRG 320 [1]; (2) the mechanical properties of the 5-layer

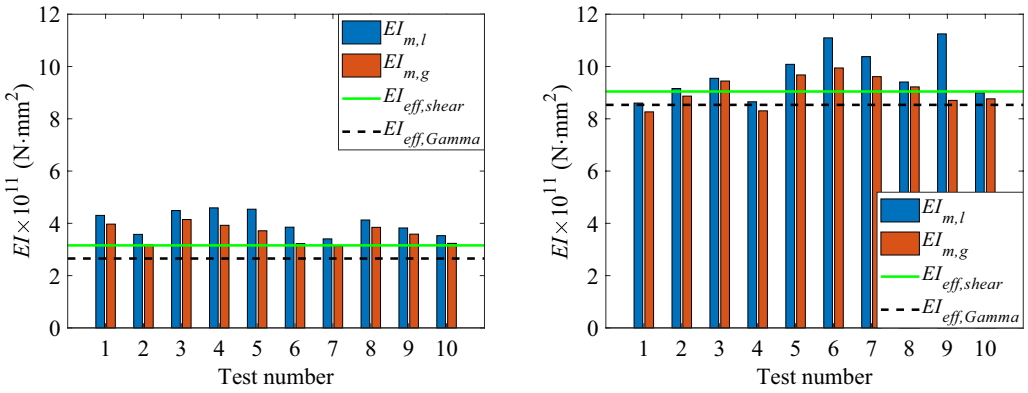

a 3-layer CLT bending specimens **b** 5-layer CLT bending specimens

Fig. 12 Bending stiffness comparison

Table 10 Mechanical properties of CLT panels fabricated with different wood species

Refs	Wood species	Thickness (mm)	No. of layers	Layups	Flexural MOE, $E_b = EI_{m,l}/I$ (MPa)	f_b (MPa)	f_v (MPa)	Features
–	Canadian black spruce	105	3	35/35/35	1.3456×10^4	30.909	1.737	Edge-glued No.2-grade lumber Made in China
–	Canadian black spruce	155	5	35/25/35/25/35	1.0204×10^4	29.633	1.803	
[1]	SPF	–	–	–	1.1700×10^4	28.200	1.500	Grade E1 defined in PRG 320 [1]
[1]	Douglas fir-Larch	–	–	–	1.0300×10^4	23.90	1.900	Grade E2 defined in PRG 320 [1]
[3]	Canadian hemlock	175	5	35/35/35/35/35	1.1671×10^4	22.422	1.605	Non-edge-glued No.2-grade lumber Made in China
[4]	Irish Sitka spruce	72	3	24/24/24	1.0247×10^4	35.550	1.710	Non-edge-glued C16-grade lumber
[4]	Irish Sitka spruce	120	3	40/40/40	0.9794×10^4	24.560	1.090	
[4]	Irish Sitka spruce	100	5	20/20/20/20/20	1.2238×10^4	33.790	1.030	
[5]	Australian Radiata pine	105	3	35/35/35	1.0246×10^4	23.410	2.000	Non-edge-glued XLG1-grade lumber for longitudinal layers; XLG2-grade lumber for transverse layers;
[5]	Australian Radiata pine	145	5	35/20/35/20/35	0.7433×10^4	26.840	1.760	
[33]	Southern pine	175	5	35/35/35/35/35	0.9202×10^4	19.980	3.040	Edge-glued No.2-grade lumber
[32]	Southern SPF & LSL	105	3	35/35/35	1.1737×10^4	33.600	2.960	Non-edge-glued Hybrid CLT No .2-grade SPF for transverse layers 1.35E-grade LSL for longitudinal layers

CLT fabricated with No.2-grade black spruce lumber are similar to those of E2-grade CLT defined in ANSI/APA PRG 320 [1], except for the f_b, which is higher than that of most CLT types (e.g., E2-grade CLT); (3) compared to the CLT panels fabricated with No.2-grade Canadian hemlock [3], the CLT panels fabricated with No.2-grade Canadian black spruce lumber can provide better bending or shear properties; (4) except for the E_b of the 3-layer black spruce CLT, the mechanical properties of those CLT fabricated with No. 2-grade black spruce lumber are less than those of the hybrid CLT manufactured by both Spruce-pine-fir (SPF) and laminated strand lumber (LSL) [32]; (5) overall, the CLT fabricated with No. 2-grade black spruce lumber can provide ideal bending or shear properties, which can be comparable to those of the CLT fabricated with other commonly used wood species.

Furthermore, in this study, edge-gluing was performed for the 3- or 5-layer CLT specimens. Compared to the edge-glued CLT panels, the in-plane shear stiffness of the non-edge-glued CLT is lower significantly [34]. More studies are required for comprehending the influence of edge-gluing on the structural performance of CLT.

Numerical model

Both the full-scale numerical model of the CLT bending specimens and that of the CLT shear specimens were developed based on ANSYS [18]. The 8-node SOLID45 element was used for simulating the black spruce lumber. The dimensions of the SOLID45 elements were defined as half of the lamination thickness (i.e., 17.5 mm or 12.5 mm). Since little de-lamination failure occurred during the aforementioned bending or shear tests, it was assumed that no slide movement occurred within the interface of the CLT neighboring laminations. Therefore, in the model of the CLT bending or shear specimens, the neighboring laminations were bonded. The orthotropic elasto-plastic performance of the spruce lumber was simulated based on the material model of HILL Plasticity combined with the model of KINH Multi-linear Kinematic Hardening. For the CLT numerical model, the material properties were assigned to each lamination of the CLT panels, based on the lumber grain orientation within this lamination. In the parallel-to-grain direction of the lumber, the tensile strength and the compressive strength were equal to f_b (i.e., 30.91 MPa for CL3/105 and 29.63 MPa for CL5/155) and equal to $f_{lc,0}$ (i.e., 28.7 MPa), respectively. In the perpendicular-to-grain direction of the lumber, the compressive strength was equal to $f_{lc,90}$ (i.e., 5.8 MPa); the tensile strength ($f_{lt,90}$) was estimated as 2.7 MPa. Since the HILL Plasticity model cannot consider the difference between tensile and compressive strengths in the same direction [35]; therefore, in the parallel-to-grain direction of the lumber, the lower of the f_b and $f_{lc,0}$ (i.e., 28.7 MPa) was adopted; meanwhile, in the perpendicular-to-grain direction of the lumber, the lower of the $f_{lc,90}$ and $f_{lt,90}$ was adopted (i.e., 2.7 MPa). Similar arrangement was also adopted by Nowak et al. [36] for the material law of glulam. The shear modulus of the longitudinal lamination (i.e., G_0) and that of the transverse lamination (i.e., G_{90}) were defined as 682.8 MPa and 68.3 MPa ($G_0 = E_{l,0}/16$, $G_{90} = G_0/10$), respectively. It should be noted that size effects of these strengths input in the numerical model were not considered in the study, which should be investigated in the future. For the models of both the CLT bending specimens and the CLT shear specimens, contour plots of their vertical deformation are shown in Fig. 13.

Both the model of the CLT bending specimens and that of the CLT shear specimens can provide accurate predictions on their initial elastic stiffness K_e, as shown in Fig. 14. For the 3-layer CLT bending specimens and for the 5-layer CLT bending specimens, their predictive F_{max} from the numerical model are respectively 30.37 kN and 36.21 kN, which are 9.94% less and 1.91% less than their average experimental F_{max}, respectively. In contrast, for the 3-layer CLT shear specimens and for the 5-layer CLT shear specimens, their predictive FV_{max} from the numerical model are respectively 45.05 kN and 58.55 kN, which are 12.76% less and 16.12% less than their average experimental FV_{max}, respectively. Therefore, compared to the predictive FV_{max} from the CLT shear model, the predictive F_{max} from the CLT bending model is more close to the average experimental F_{max}. For these CLT shear specimens, their FV_{max} can be underestimated significantly, when using the developed model of the CLT shear specimens. It is because the experimental FV_{max} can still remain increasing after slight rolling shear failure occurring in the CLT shear specimens; whereas the mechanism of the rolling shear failure cannot be reflected in the developed model. Future efforts should focus on developing a numerical model of CLT shear panels that can consider the influence of the rolling shear mechanism.

Conclusions

Based on the experimental investigation and theoretical analysis on both the bending and the shear properties of black spruce CLT panels, the conclusions can be drawn as follows:

(1) For the CLT bending panels, increasing the CLT thickness whilst maintaining identical span-to-thickness ratios can even slightly reduce their characteristic bending strength f_b. Besides, for the CLT shear panels, increasing the CLT thickness whilst maintaining identical span-to-thickness ratios has little enhancement on their characteristic shear strength f_v.
(2) For both the 3-layer and the 5-layer CLT bending panels, their effective bending stiffness based on the Shear Analogy theory can be used as a more accurate prediction on their experiment-based global bending stiffness.
(3) The dominant failure mode of the CLT bending specimens is the brittle tension failure occurring in the CLT bottom longitudinal lamination; whereas, that of the CLT shear specimens is the rolling shear failure occurring in the transverse laminations.
(4) Both the 3-layer and the 5-layer CLT panels fabricated with the No.2-grade black spruce can provide ideal bending or shear properties, which can

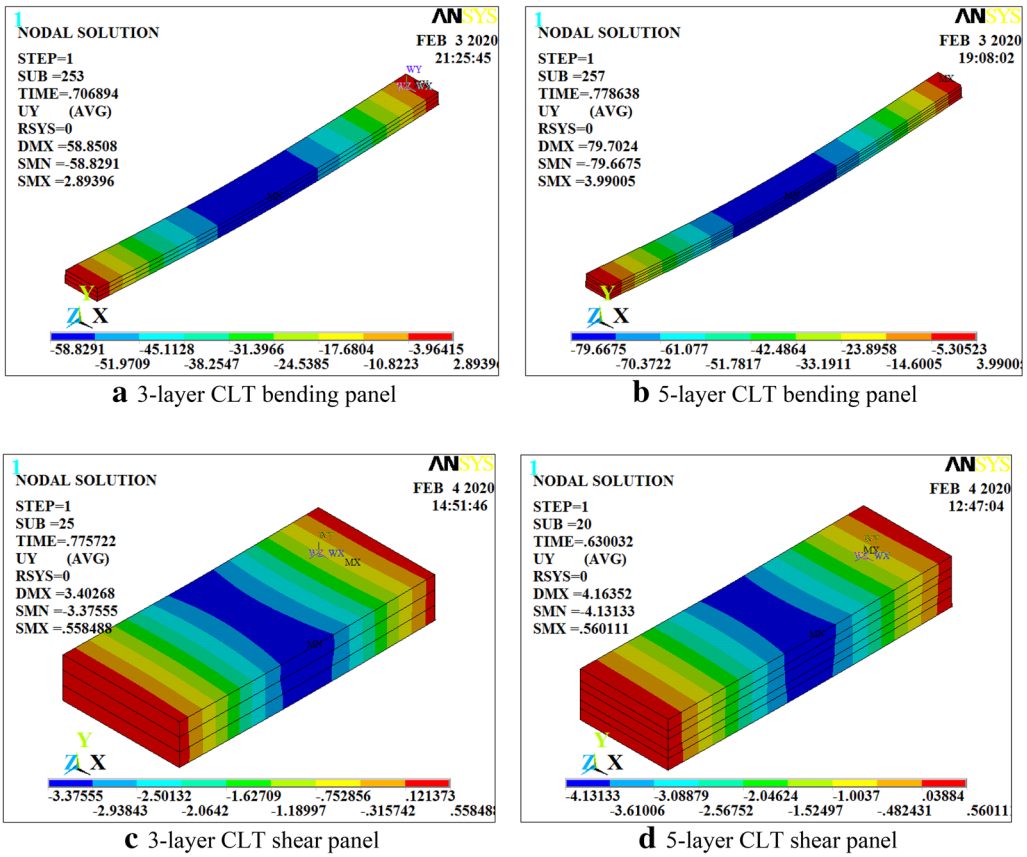

Fig. 13 Contour plots of the vertical deformation from the models

be comparable to those of the CLT fabricated with other commonly used wood species.

(5) The numerical model of the CLT bending specimens is capable of predicting both their initial elastic stiffness K_e and their ultimate load-resisting capacity $F_{\max}$. Whereas, based on the numerical model of the CLT shear specimens that cannot reflect the rolling shear mechanism, the initial elastic stiffness K_e can be predicted accurately but the ultimate shear-resisting capacity $FV_{\max}$ is underestimated.

List of symbols

$E_{l,0}$: Modulus of elasticity of the lumber in parallel-to-grain direction; $E_{l,90}$: Modulus of elasticity of the lumber in perpendicular-to-grain direction; $E_{c3,0}$: Modulus of elasticity of the 3-layer CLT panels in major in-plane compressive direction; $E_{c3,90}$: Modulus of elasticity of the 3-layer CLT panels in minor in-plane compressive direction; $E_{c5,0}$: Modulus of elasticity of the 5-layer CLT panels in major in-plane compressive direction; $E_{c5,90}$: Modulus of elasticity of the 5-layer CLT panels in minor in-plane compressive direction; $f_{lc,0}$: Compressive strength of the lumber in the parallel-to-grain direction; $f_{lc,90}$: Compressive strength of the lumber in the perpendicular-to-grain direction; $f_{c3,0}$: In-plane major compressive strength of the 3-layer CLT panels; $f_{c3,90}$: In-plane minor compressive strength of the 3-layer CLT panels; $f_{c5,0}$: In-plane major compressive strength of the 5-layer CLT panels; $f_{c5,90}$: In-plane minor compressive strength of the 5-layer CLT panels; $EI_{m,l}$: Local bending stiffness of CLT bending panels; $EI_{m,g}$: Global bending stiffness of CLT bending panels; $F_{\max}$: Ultimate load-resisting capacity of CLT bending panels; GA_{eff}: Effective shear stiffness of CLT panels; G_0: Shear modulus parallel to grain for CLT longitudinal laminations; G_{90}: Rolling shear modulus for CLT transverse laminations; h: Total thickness of CLT panels; h_i: The thickness of CLT lamination i; E_i: Modulus of elasticity of CLT lamination i; E_1: Modulus of elasticity of the CLT outer most lamination; f_b: The characteristic bending strength of CLT bending panels (i.e., characteristic bending strength of the CLT outermost lamination); S_{eff}: The effective section modulus of CLT panels; K_e: Initial elastic stiffness obtained from the load–displacement curves; $FV_{\max}$: Ultimate shear resisting capacity of CLT shear panels; f_v: The characteristic shear strength of CLT shear panels; EI_{eff}: The effective bending stiffness of CLT bending panels; $EI_{\text{eff,shear}}$: The effective bending stiffness calculated based on the Shear Analogy theory; $EI_{\text{eff,Gamma}}$: The effective bending stiffness calculated based on the Modified Gamma theory; f_r: The characteristic rolling shear strength; γ_i: The connection efficiency factor for CLT longitudinal laminations; E_b: Flexural modulus of elasticity of the CLT bending specimens.

Acknowledgements
Not applicable.

Authors' contributions
MH: conceptualization, methodology, and investigation. XS: data curation, methodology, investigation, software, and writing–review and editing. ZLi: conceptualization, methodology, and investigation. WF: software and validation. All authors read and approved the final manuscript.

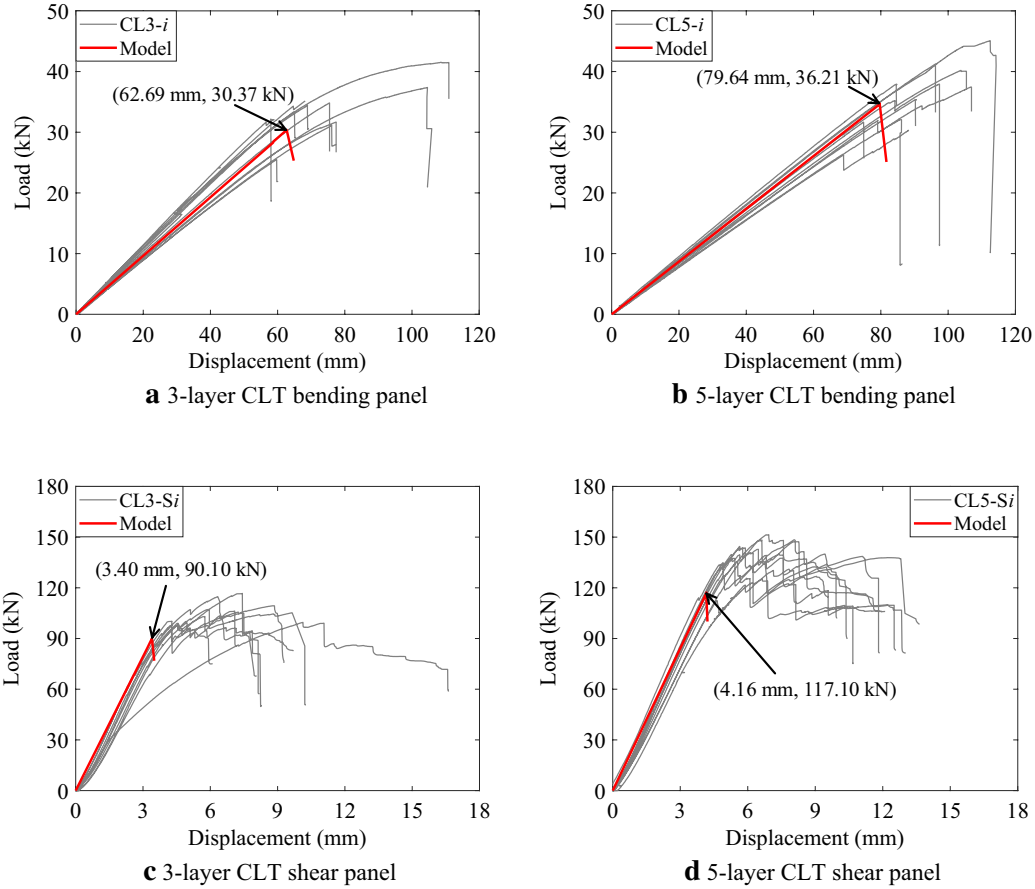

Fig. 14 Comparisons between experimental curves and numerical curve

Funding
The authors also gratefully acknowledge the support from National Natural Science Foundation of China (Grant NO. 51778460) and China Scholarship Council (Grant NO. 201706260124).

Availability of data and materials
The datasets used and/or analyzed during the current study are available from the corresponding author on reasonable request.

Ethics approval and consent to participate
Not applicable.

Consent for publication
Not applicable.

Competing interests
There is no competing interests.

Received: 21 February 2020 Accepted: 8 May 2020
Published online: 19 May 2020

References

1. ANSI/APA PRG 320, (2018) Standard for performance-rated cross laminated timber. APA-The Engineered Wood Association, Tacoma
2. Sun XF, He MJ, Li Z (2020) Novel engineered wood and bamboo composites for structural applications: state-of-art of manufacturing technology and mechanical performance evaluation. Constr Build Mater 249:118751
3. He MJ, Sun XF, Li Z (2018) Bending and compressive properties of cross-laminated timber (CLT) panels made from Canadian hemlock. Constr Build Mater 185:175–183
4. Sikora KS, McPolin DO, Harte AM (2016) Effects of the thickness of cross laminated timber (CLT) panels made from Irish Sitka spruce on mechanical performance in bending and shear. Constr Build Mater 116:141–150
5. Navaratnam S, Christopher PB, Ngo T, Le TV (2020) Bending and shear performance of Australian Radiata pine cross-laminated timber. Constr Build Mater 232:117215
6. Li M (2017) Evaluating rolling shear strength properties of cross-laminated timber by short-span bending tests and modified planar shear tests. J Wood Sci 63(4):331–337
7. Ukyo S, Shindo K, Miyatake A (2019) Evaluation of rolling shear modulus and strength of Japanese cedar cross-laminated timber (CLT) laminae. J Wood Sci 65(1):31
8. Oh JK, Lee JJ, Hong JP (2015) Prediction of compressive strength of cross-laminated timber panel. J Wood Sci 61(1):28–34
9. Ido H, Nagao H, Harada M, Kato H, Ogiso J, Miyatake A (2016) Effects of the width and lay-up of sugi cross-laminated timber (CLT) on its dynamic and static elastic moduli, and tensile strength. J Wood Sci 62(1):101–108

10. Chen ZY, Zhu EC, Pan JL (2011) Numerical simulation of wood mechanical properties under complex state of stress. Chin J Comput Mech 28(04):629–634
11. Chen ZY, Ni C, Dagenais C, Kuan S (2020) Woodst: a temperature-dependent plastic-damage constitutive model used for numerical simulation of wood-based materials and connections. J Struct Eng 146(3):04019225
12. Ceccotti A (2008) New technologies for construction of medium-rise buildings in seismic regions: the XLAM case. Struct Eng Int 18(2):156–165
13. Franco L, Pozza L, Saetta A, Savoia M, Talledo D (2019) Strategies for structural modelling of CLT panels under cyclic loading conditions. Eng Struct 198:109476
14. D'Arenzo G, Casagrande D, Reynolds T, Fossetti M (2019) In-plane elastic flexibility of cross laminated timber floor diaphragms. Constr Build Mater 209:709–724
15. Wilson AW, Motter CJ, Phillips AR, Dolan JD (2019) Modeling techniques for post-tensioned cross-laminated timber rocking walls. Eng Struct 195:299–308
16. Sun XF, He MJ, Li Z (2019) Seismic performance assessment of conventional CLT shear wall structures and post-tensioned CLT shear wall structures. Eng Struct 196:109285
17. Hashemi A, Masoudnia R, Quenneville P (2016) A numerical study of coupled timber walls with slip friction damping devices. Constr Build Mater 121:373–385
18. Kohnke P (1999) ANSYS Theory Manual—Release 57. Canonsburg, ANSYS
19. Popovski M, Gagnon S, Mohammad M, Chen ZY (2019) Chapter —structural design of cross-Laminated timber elements. CLT Handbook, 2nd edn. FPInnovations, Vancouver, pp 1–56
20. NLGA (2010) Standard grading rules for Canadian lumber. National Lumber Grades Authority, Surrey
21. Karacebeyli E, Gagnon S (2019) Canadian CLT Handbook, 2nd edn. FPInnovations, Vancouver
22. GB/T 26899–2011 (2011) Structural glued laminated timber. China's National Standard, Beijing
23. GB/T 50329–2012 (2012) Standard for test methods of timber structures. China's National Standard, Beijing
24. PrEN 16351 (2013) Timber structures—Cross laminated timber-requirement. European Committee for Standardization, CEN
25. EN 408 (2012) Timber structures—Structural timber and glued laminated timber-determination of some physical and mechanical properties. European Committee for standardization, CEN, Bruxelles, Belgium
26. Chen Z, Popovski M, Symons P (2018) Advanced wood-based solutions for mid-rise and high-rise construction: Structural performance of post-tensioned CLT Shear Walls with Energy Dissipators. FPInnovations Project (No. 301012204) Report: Vancouver
27. Christovasilis IP, Brunetti M, Follesa M, Nocetti M, Vassallo D (2016) Evaluation of the mechanical properties of cross-laminated timber with elementary beam theories. Constr Build Mater 122:202–213
28. Thiel A, Schickhofer G (2010) CLT designer—a software tool for designing cross-laminated timber elements: 1D-plate-design. In: WCTE 2010—11th World Conference on Timber Engineering, Riva del Garda
29. EN 338 (2009) Structural timber—Strength classes. European Committee for standardization, CEN, Bruxelles, Belgium
30. Blass HJ, Fellmoser P (2004) Design of solid wood panels with cross layers. In: WCTE 2004—8th World Conference on Timber Engineering, Lahti, Finland
31. EN 1995, Eurocode 5 (2008) Design of timber structures-part 1–1: general-common rules and rules for buildings. European Committee for Standardization, CEN, Bruxelles
32. Davids WG, Willey N, Lopez-Anido R, Shaler S, Gardner D, Edgar R, Tajvidi M (2017) Structural performance of hybrid SPFs-LSL cross-laminated timber panels. Constr Build Mater 149:156–163
33. Hindman DP, Bouldin JC (2015) Mechanical properties of southern pine cross-laminated timber. J Mater Civil Eng 27:4014251
34. Berg S, Turesson J, Ekevad M, Bjornfot A (2019) In-plane shear modulus of cross-laminated timber by diagonal compression tests. BioResources 14(3):5559–5572
35. Chen Z, Ni C, Dagenais C (2018) Advanced wood-based solutions for mid-rise and high-rise construction: modelling of timber connections under force and fire. FPInnovations Project (No. 301012203) Report: Vancouver
36. Nowak TP, Jasienko J, Czepizak D (2013) Experimental tests and numerical analysis of historic bent timber elements reinforced with CFRP strips. Constr Build Mater 40:197–206

Publisher's Note